

New Mechanism for a 3 DOF Exoskeleton Hip Joint with Five Revolute and Two Prismatic Joints

Jonas Beil and Tamim Asfour
Institute for Anthropomatics and Robotics
Karlsruhe Institute of Technology, Karlsruhe, Germany

Abstract—We present a new exoskeleton hip design representing the human hip ball joint by five revolute and two prismatic joints. The goal of the design is to increase wearing comfort and torque transmission by reducing misalignments between the human’s and the exoskeleton’s joint with a self-aligning yaw axis in the transverse plane. The required ranges of motions and joint velocities for the hip joint design were identified based on motion capture data consisting of 828 motion recordings of 26 different subjects. We present the kinematics of a new hip joint with five revolute and two prismatic joints and its first 3D printed prototype. For the experimental evaluation we focused on measuring interaction forces between the subject and the exoskeleton at the back, pelvis and thigh with different kinematic configurations. The results indicate that interaction forces between exoskeleton and user are reduced by the new hip exoskeleton.

I. INTRODUCTION

Recently, considerable research efforts have been made in the area of exoskeleton development to augment human performance in daily and working environments. When designing such systems, wearability and comfort are key requirements which must be addressed to enhance the acceptance of such assistive devices by their wearer. Application scenarios in daily living or working activities demand devices that can be used for hours without discomfort or skin abrasions caused by micro or macro misalignments between the user and the exoskeleton hip axes [1].

A self-aligning design using supplementary joints is therefore beneficial to adjust the exoskeleton joint axis with the users hip instantaneous centers of rotation (ICR). Misalignments occurring at the hip also propagate to the knee and ankle joints or vice versa and decrease the efficiency of actuators and interfaces. To this end, it is important to design misalignment-free hip joints for lower limb exoskeletons. In this work, we present a novel design for an exoskeleton hip joint which allows such adjustments.

Exoskeletons like Mina [2], eLegs [3] or HAL [4] only have either one degree of freedom (DOF) for hip flexion/extension or two DOF adding hip abduction/adduction. Other devices like the Mindwalker exoskeleton [5], the lower body exoskeleton presented in [6] or the XOR2 [7] add a revolute joint between the roll and pitch joint to support hip rotation, accepting macro misalignments between the ICRs for this DOF. This macro misalignment is reduced in designs like the IHMC mobility assist exoskeleton [8] or the BLERE [9], which use a curved bearing to locate the center of rotation



Fig. 1. 3D printed prototype of the proposed hip joint of a lower limb exoskeleton

approximately at the user’s hip joint. Pons [10] and Cempini et. al. [11] propose additional joints to create self-aligning wearable devices that are comfortable and easy to use. The inter-subject variability of the human musculo-skeletal system, articulation and soft tissue deformation impede device designs that correctly align the axis of the human body and the mechanism.

Usually, macro misalignments are reduced by manual adaptable mechanism to regulate link length and are combined with flexible attachments or additional passive joints at the physical Human Robot Interface (pHRI). In [12], the authors added a passive sliding and rotational adjustment to an orthotic shell, interfacing an assistive hip orthosis with the users thigh. Supplementary joints are also used in exoskeleton devices for the upper body to self-align the wrist and forearm joints [13] or the elbow [14]. This paper presents a hip exoskeleton structure using supplementary joints to self-align to the user yaw axis in the transverse plane and aims to be integrated in an augmenting assistive device. Section II describes the requirements for the system resulting from human hip anatomy and human motion analysis. Section III explains the chosen kinematics and design of the prototype. Experimental evaluation of the design with different kin-

matic configurations and the force-based sensor system for measuring interaction forces between the exoskeleton and the user are presented in Section IV. Section V concludes the paper.

II. DESIGN REQUIREMENTS OF A HIP EXOSKELETON

The human hip joint is a ball and socket joint with convex on concave or concave on convex movement characteristics [15]. Translational motions between the femoral head and the acetabulum is minimized by the bone structure and soft tissue support when rotating in the sagittal, transverse or frontal plane. Though the translational motions are very small, differences in the musculoskeletal system as well as other inter-subject body characteristics (height, body mass index, age) should be compensated by a flexible mechanical design. According to the German DIN Norm [16], the 5 to 95 percentile of hip width of adults aged between 18 and 65 amount 340 to 400 *mm* when standing and 350 to 460 *mm* while sitting. Considering exoskeleton design, easy to manipulate mechanisms compensating body width and height in the transverse and frontal body plane have to be included for offline adjustment.

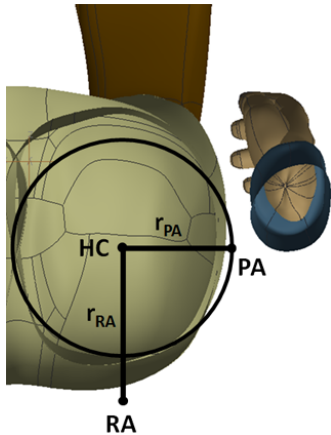


Fig. 2. Assumptions for hip rotation in transverse plane (top view).

When rotating the leg in the transverse plane, we assume that the point at the outside pelvis created by the pitch axis and the pelvis skin (PA) performs a circular movement with center HC, radius r_{PA} and angle ϕ which should also be performed by the exoskeleton yaw axis. If the yaw joint mechanism is not positioned after the pitch joint like in [9] but between roll and pitch, application points at the back (RA) and the side pelvis (PA) vary from user to user (see Figure 2). Therefore, it is important for the design to allow positioning the pitch joint's center of rotation such that the equations in Equation (1) are fulfilled. Assembling the yaw mechanism at the leg could constrain future knee joint mechanisms or attachment points of actuators and is therefore avoided in this work.

$$\begin{aligned} PA_x &= HC_x + r_{PA} \cdot \cos(\phi) \\ PA_y &= HC_y + r_{PA} \cdot \sin(\phi) \end{aligned} \quad (1)$$

Human hip maximum range of motion (ROM) reach up to 20/90° for flexion/extension, 40/25° for abduction/adduction and 35/45° for internal/external rotation [15]. However, the joint angles are smaller during walking or most activities of daily living or working. This affects the device design and the maximum displacement of linear actuators as well as their positioning regarding the resulting torque arm. Therefore, joint angles and joint velocities during activities like walking forward or backwards, right/left turning and walking on stairs or slopes have to be investigated to derive the required ranges of motions for the three hip joints. Data from motion recordings with a 10 camera VICON (Vicon Motion Systems) system available in the KIT Motion Data Base [17] were used to support our design of the new hip joint. Table I summarizes the information regarding the type and characteristics of motions, the number of subjects and the number of motions we used in our analysis.

TABLE I
SUBJECTS AND MOTIONS

Motion	Velocity	Subjects	Motions	Size [m]
Walk forward	fast	5	45	1.63 - 1.86
Walk forward	medium	14	137	1.63 - 1.92
Walk forward	slow	9	80	1.63 - 1.86
Walk backward	medium	8	78	1.6 - 1.92
Turn left	medium	16	149	1.63 - 1.92
Turn right	medium	14	134	1.64 - 1.92
Walk upward	medium	20	106	1.63 - 1.86
Walk downward	medium	19	98	1.63 - 1.86
Total	-	26	828	-

The desired ROMs of the three hip joints were gathered by processing the motion data with MATLAB. Every motion was performed multiple times by one subject thus the maximum hip joint angles are first calculated subject-wise by calculating the 2 and 98 percentile of every single motion to prevent unrealistic joint angles occurring to outliers in the data. Then the maximum joint angle values of all users and of the left and right leg were compared to get the final ROMs (Table II). The same procedure was executed for the joint velocities which are numerically derived from the joint angles given in Table III.

TABLE II
RANGE OF MOTION IN THE HUMAN MOTION DATA

Motion	Roll [°]	Yaw [°]	Pitch [°]
Walk forward fast	-8.8 - 12.3	-6.3 - 7.8	-14.8 - 48.4
Walk forward medium	-6.7 - 9.5	-7.7 - 8.7	-10.4 - 40.3
Walk forward slow	-6.2 - 11.9	-4.9 - 6.0	-9.7 - 36.2
Walk backward	-5.5 - 6.9	-3.2 - 3.9	0.7 - 43.4
Turn left	-7.9 - 11.3	-8.6 - 13.6	-6.8 - 41.7
Turn right	-8.1 - 10.4	-8.4 - 10.3	-8.1 - 45.7
Walk upward	-7.5 - 13.4	-8.8 - 10.9	-3.2 - 70.1
Walk downward	-6.3 - 12.5	-10.5 - 11.3	-2.9 - 45.9

TABLE III

REQUIRED JOINT VELOCITIES CALCULATED FROM THE MOTION DATA

Motion	Roll	$\frac{rad}{s}$	Yaw	$\frac{rad}{s}$	Pitch	$\frac{rad}{s}$
Walk forward fast	-1.14 – 0.93		-1.54 – 1.34		-2.80 – 3.75	
Walk forward medium	-0.75 – 0.86		-1.33 – 1.31		-1.61 – 2.65	
Walk forward slow	-0.68 – 0.65		-0.78 – 0.87		-1.08 – 1.99	
Walk backward	-0.58 – 0.48		-0.53 – 0.50		-2.08 – 1.17	
Turn left	-1.07 – 0.75		-1.85 – 1.73		-1.61 – 2.73	
Turn right	-0.78 – 0.88		-1.67 – 1.51		-1.62 – 2.59	
Walk upward	-0.70 – 0.92		-1.27 – 1.19		-2.06 – 3.07	
Walk downward	-0.94 – 0.92		-1.49 – 1.46		-1.91 – 2.15	

A Positive roll angle corresponds to hip abduction, positive yaw angle to external rotation and positive pitch angle to hip flexion. Gait speed was determined by the recorded subject who was asked to perform a fast, medium or slow walking motion. The analysis indicates the broad range of angles between different motions and summarizes to $-8.8 - 13.4^\circ$ for the roll, $-10.5 - 13.6^\circ$ for the yaw and $-14.8 - 100^\circ$ (to allow sitting with the exoskeleton) for the pitch DOF. The joint velocities vary from $-1.14 - 0.93 \text{ rad/s}$, $-1.85 - 1.73 \text{ rad/s}$ and $-2.8 - 3.75 \text{ rad/s}$ in the aforementioned directions. The hip joint construction should meet at least the ROMs derived from the analysis.

In our design, we envision a rate of assistance of half body weight of a 80 kg person per leg, i.e. 40 kg , which leads to expected torques of 50 Nm in frontal plane, 8 Nm in transverse plane and 60 Nm in sagittal plane according to [15].

III. DESIGN OF THE HIP EXOSKELETON

A. Kinematics

To fulfill the requirements derived in section II a non-anthropomorphic exoskeleton kinematic structure is proposed, consisting of revolute joints in the roll and pitch axis and a combination of three revolute and two prismatic joints for the yaw axis. The kinematics are schematically illustrated in Figure 3 and are described in standard Denavit-Hartenberg (DH) parameters shown in Table IV. Origin O is the beginning of the chain, and is positioned on the sagittal plane of the human on the back plate which is connected to the backpack (Stihl RTS-HT, Waiblingen) worn by the user. Coordinate system L_9 coincides with the last link connecting the exoskeleton to the users thigh.

The roll axis is aligned by hand using eccentric clamps (Heinrich Kipp Werk KG, Sulz am Neckar), adjusting the position of L_1 in frontal and transverse plane according to the range specified in Section II. A high precision double row angular ball bearing (30/85 2RS, SBN Wälzlager GmbH & Co. KG, Schöenberg-Kübelberg) simultaneously captures thrust and radial loads and is used in all revolute joints of the hip design. Taking motion analysis into account the ROM of the roll joint is limited to $\pm 20^\circ$.

The yaw joint ($L_3 - L_7$) is designed as a serial chain of three revolute and two prismatic (LWRE 3075, SKF GmbH,

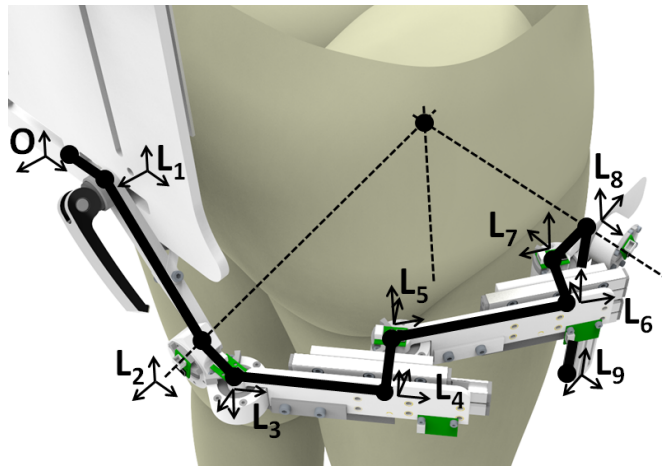


Fig. 3. Kinematic structure with coordinate systems in the different joints, which are used to determine the DH-parameter.

TABLE IV
DH PARAMETERS OF THE HIP DESIGN

Link	Angle θ_i	Twist α_i	Length a_i	Disp d_i
L1	0	0	0	$34.5 + d_1$
L2	-90°	90°	74.5	62.5
L3	$90^\circ + \theta_3$	-90°	31.5	0
L4	$90^\circ + \theta_4$	90°	0	0
L5	0	-90°	30.5	$97.5 + d_5$
L6	θ_6	90°	0	0
L7	0	-90°	30.5	$97.5 + d_7$
L8	$-90^\circ + \theta_8$	90°	37.5	0
L9	$90^\circ + \theta_8$	0	80	0

Schweinfurt) joints around the user's body to guarantee a flexible device which can be worn by a broad range of people with different body dimensions, hip kinematics and articulation. The combination of revolute and prismatic joints allows the positioning of the pitch axis moving on a circle around the hip center.

Due to the low maximum torque (0.2 Nm/kg) and power (0.16 W/kg) [15] during walking, we believe that actuation of the joint is not essential but passive parallel elastic elements at the prismatic bearings can support the user while walking. The first prototype therefore uses springs connected at both ends of the prismatic bearings, applying force in direction of their zero position preventing uncontrolled joint movement and apply a small amount of torque contrary to propelling torque. Although the prototype is not actuated yet, the prismatic and revolute bearings were chosen to support the loads resulting of a weight of 80 kg .

To derive the ROM for the yaw joint, the DH-parameters were used to reach the position of PA (calculated with Equation 1) with angles between $10 - 60^\circ$ for θ_3 , θ_5 and θ_7 and a displacement of $0 - 60 \text{ mm}$ for d_4 and d_6 using MATLAB. Allowing free movement of all revolute joints leads to indefinite kinematics resulting in multiple joint configurations for one position of PA. Taking different human body characteristics into account, radius r_{PA} was increased

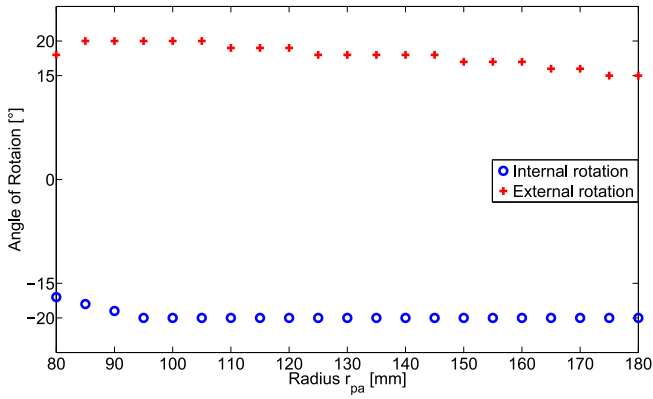


Fig. 4. Calculated range of motion of the exoskeleton hip yaw axis varying r_{PA} .

starting from 80 mm until the minimum joint angle crosses $\pm 15^\circ$ or over $\pm 20^\circ$ and calculation is stopped when one possible joint configuration is found. Fig. 4 presents the resulting ROM when increasing r_{PA} from 80 – 180 mm, demonstrating the design flexibility.

The pitch joint (L_8) consists of the aforementioned double row angular ball bearing and has a ROM of $-20 - 100^\circ$. Alignment to the users pitch axis in transverse plan when donning the device is obtained by the yaw mechanism.

B. Actuation and Torque Admissibility

As mentioned before the roll and pitch joints should be actuated with linear actuators. Figure 5 illustrates the actuator setup and their mounting points AM_{1-4} which are provided to allow actuator forces up to 1000 N. Torque transmission over L_7 demands for a locking mechanism in that joint, which is provided by a gearing that allows stepping of 7° . When donning the exoskeleton gears are disengaged allowing rotation in the joint and adaption of the device to the user's body. Torque transmission is obtained by fastening a screw (engaging the gears) after donning is complete.

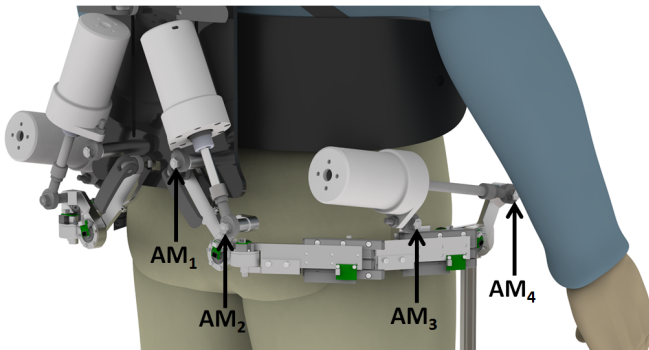


Fig. 5. Actuation setup for the hip exoskeleton

The maximum torque arm of a linear actuator mounted between AM_3 and AM_4 is 60 mm resulting in a maximum joint torque of 60 Nm at a joint flexion angle of 30° corresponding to the angle with highest torque in the gait cycle. When sitting (90° flexion), a torque of 58 Nm is

possible in pitch direction. Maximum torque arm for the roll joint is 50 mm resulting in maximum torque of 50 Nm at 0° . The mounting points were chosen by calculating torque arm progression over the joints ROM, maximizing the torque and maintaining the joint's angular velocity when walking at 5 km/h.

Torque admissibility of the exoskeleton is investigated with FEM-Analysis. In the first case, forces of 1000 N are exerted on the actuator mounting points and the exoskeleton joints L_2 and L_8 are restrained. This corresponds to the case when the human prevents exoskeleton movement while the actuators exert maximum force and the resulting maximum von Mises stress is 168.5 MPa with maximum displacement of 0.09 mm.

In the second case the user exerts torques of 100 and 120 Nm on the pitch and roll axis while the self locking actuators resist that movement. This increases the maximum von Mises stress to 231.8 MPa and maximum displacement to 0.12 mm.

C. Sensor Setup and Prototype

Angular positions are measured by 12 bit absolute encoders (AS5145B, ams AG, Premstaetten) which are processed by an ATmega 32 (Atmel Corporation, San Jose). The same microcontroller also processes the signals of the linear position encoders on the prismatic bearings (AS 5306B, ams AG, Premstaetten).

To test the kinematics on a real user, a 3D printed prototype, shown in Fig. 1 was assembled using the proposed bearings and sensors. Some parts had to be slightly redesigned or reinforced by aluminum beams to prevent bending of the system while moving. The system is mounted on a backpack with a pelvis belt to secure it on the users upper body. Velcro straps hold the system at the thigh.

IV. EVALUATION AND RESULTS

As stated in Section I discomfort from wearing an exoskeleton is often the result of misaligned ICRs which causes pressure and shear forces on the users skin. Our evaluation therefore concentrates on the measurement of the forces between user and exoskeleton measuring shear forces on the user's pelvis and pressure forces on back, pelvis and thigh while performing the motions described in Section II. Though the exoskeleton is not in contact with the user at the side pelvis, force measurement can indicate exoskeleton movement relative to the body.

Pressure forces at the back (S1) and thigh (S4) are gathered with ELAF B0 1D force sensors (Measurement Specialties, Hampton) integrated in a 3D printed interface to ensure orthogonal force influence. Shear (S3) and pressure (S2) forces applied to the users pelvis are measured by a combination of the aforementioned ELAF sensor and a second compression-tension sensor (XFTC 301, Measurement Specialties, Hampton) placed orthogonally to S2. Both sensors are integrated in one 3D printed interface as illustrated in Figure 7.

The shape of the interface forms two springs transferring load to the sensors. A quadratic model compensates interfering forces on the sensors caused by the coupling of force

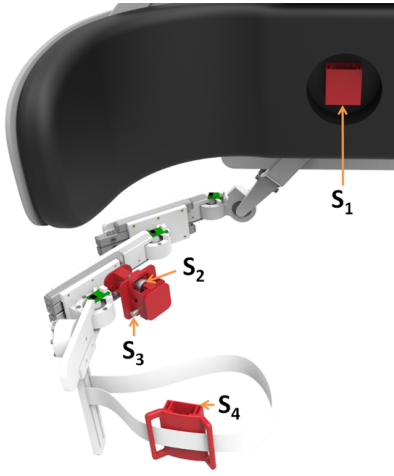


Fig. 6. The developed sensor setup to evaluate shear and compression forces between the user and the exoskeleton.

directions. A ball joint (EGLM-10, igus GmbH, Köln) in the base of the device aligns the top surface to the user's body. Fig. 6 presents the complete sensor setup, where all sensor interfaces are rendered in red.

The subject had to perform a predefined set of motions (two steps forward, turn right in two steps, turn left in two steps, walk two steps backward) while wearing the exoskeleton. Prior to the first trials the subject had a short period of time to become familiar with the device and three trials were performed in the first phase with all joints unlocked at a speed determined by the subject. In the second phase the same motions were performed with joint L_5 (the revolute joint in between the two prismatic bearings) locked at the angle engaging when the subject was standing relaxed in upright position. Subsequent trials were performed with joints L_3 , L_5 and L_7 locked and in the last phase joints $L_3 - L_7$ were fixed.

The force data as well as the orientation of two inertial measurement units (IMU) attached on the backpack at L_0 and on the thigh at L_9 are processed in MATLAB. The data is smoothed by a moving average and the mean of all maximum force values corresponding to a sensor and a phase

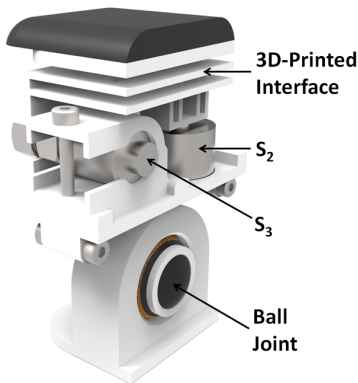


Fig. 7. 3D printed sensor interface to measure shear and compression forces simultaneously (cross sectional rendering).

(e.g. all joints unlocked) are calculated. Positive force values correspond to compression forces on sensors S_1 , S_2 and S_4 or to a shear force towards L_6 on sensor S_3 . A data set with all joints unlocked is shown in Fig. 8. The repeating force peaks indicate heel strike while walking.

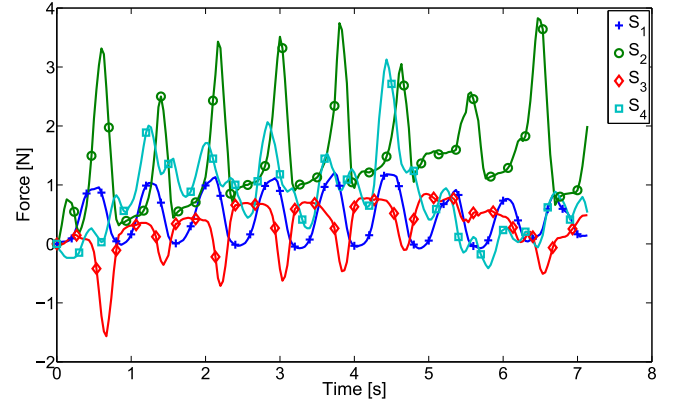


Fig. 8. Recorded force data of one trial to evaluate the exoskeleton with unlocked joints.

To compare the force data recorded in phase 1 – 4 the 5 and 95 percentile of the data sets were calculated to gather maximum and minimum sensor values per trial. Prior to each trial the inter-subject sensor values were adjusted by tightening the thigh and back straps when subjects were standing in an upright relaxed pose. Two subjects performed three trials per phase using the aforementioned procedure. The mean of the three maximum and minimum values per phase is used to compare force data between the phases. Table V lists maximum and minimum values of each sensor for phase 1 – 4. Negative values of sensor S_3 correspond to shear forces towards L_6 .

TABLE V
MAXIMUM FORCE VALUES RECORDED DURING EXPERIMENTS WITH TWO SUBJECTS

Phase	S_1 [N]	S_2 [N]	S_3 [N]	S_4 [N]
1	0.25–1.52	1.65–5.13	-1.49–0.82	3.19–5.23
2	0.33–1.54	1.14–7.28	-3.67–0.17	1.42–3.25
3	0.52–1.83	2.78–8.47	-3.06–0.62	4.40–6.28
4	0.42–1.81	3.14–8.19	-2.67–0.78	5.79–7.91

The data indicates increasing forces between the hip construction (S_2 and S_3) and the user if joints are locked. Compression forces on S_2 have higher maximum and minimum values indicating higher peak loads on the user's body for a longer period of time during phases 3 and 4. In phase 2 peak forces also increase compared to phase 1 but minimum forces remain on the same level. The shear forces towards L_6 approximately double when locking any joints of the exoskeleton. This corresponds to the observations in phase 3 and 4 of S_2 .

In phase 2 the highest shear forces and low thigh forces arise which is contrary to sensor values in the other phases

and can be explained with changed gait characteristics because the subjects expecting major changes of the exoskeletons behavior when told that one joint is locked. Also, the locking procedure could be responsible for the measurements. Locking is done when the user stands relaxed in upright position and any joint angle between 10–40 ° is accepted which could affect forces during gait. Pelvis and thigh forces increase in phase 3 and 4 with the number of joints locked while indicating misalignment between the device and the user. Discomfort depends on the maximum force and duration. The percentage values from the comparison of trials while forces exceed the maximum force occurring in phase 1 is shown in Table VI.

TABLE VI
FORCES EXCEEDING PHASE 1 MAXIMUM VALUES

Phase	S_1	S_2	S_3	S_4
1	0	0	0	0
2	0.14	0.23	0.48	0
3	0.13	0.54	0.11	0.14
4	0.10	0.52	0.06	0.18

The comparison indicates higher compression forces on the user’s hip during 10% and higher shear forces during 23 – 54% of the trials. Pelvis forces are increased during 6 – 48% of gait cycle. Forces on the thigh in phase 3 and 4 exceed phase 1 forces during 14 – 18 % of trials. In phase 2, forces were always lower than in phase 1.

Joint angle data was measured with 2 IMUs as described before and are trending towards zero for the yaw DOF when locking more and more joints. Also the maximum angle for the pitch DOF decreases slightly (4 – 9%) when moving with locked joints. The roll joint is not affected by the locking.

The results indicate the positive effects resulting from adding redundant joints to the exoskeleton hip between the roll and pitch joints. To gather a more detailed picture of the effects additional experiments with a larger number of subjects have to be performed. A prototype with a more stiff structure (manufactured from aluminum and steel) should be assembled to prevent increased bending of the design.

V. CONCLUSIONS AND FUTURE WORK

We presented a first prototype of a 3 DOF exoskeleton hip consisting of five revolute and two prismatic joints to align the exoskeleton to different body characteristics and decrease misalignments of the yaw ICR between the human and exoskeleton joint axis. The required ROMs and joint velocities were obtained by analyzing 828 human motion recordings of 26 different subjects performing eight different motions. The mechanical design consists of a serial chain with five revolute and two prismatic joints and can be aligned to different body heights and width with eccentric clamps.

Our analysis proved sufficient mobility of the system to perform the motions we considered. The experimental evaluation of the proposed design focused on measuring the compression and shear forces between exoskeleton and

subject at three positions. Our first experiments with a 3D-printed prototype indicate a benefit of redundant joints in the hip design regarding the reduction of interaction forces on the subject’s hip, pelvis and thigh while performing walking motions.

In the future the experiments will be pursued with a more stiff prototype including an enhanced sensor setup and more comprehensive analysis regarding the number and type of human motion data as well as the number of subjects. Inadvertent bending of the structure can potentially falsify the results and should be further investigated. The integration of actuators driving the roll and pitch joint of the system as well as elastic elements parallel to the prismatic joints is one of the next steps in our work. Additional passive joints on the interfaces at back and thigh can lead to self-alignment of the device in all anatomical planes.

REFERENCES

- [1] A. Schiele, *Fundamentals of ergonomic exoskeleton robots*. TU Delft, Delft University of Technology, 2008.
- [2] P. D. Neuhaus *et al.*, “Design and evaluation of mina a robotic orthosis for paraplegics,” in *2011 IEEE International Conference on Rehabilitation Robotics Rehab Week Zurich, ETH Zurich Science City, Switzerland, June 29 - July 1, 2011*. IEEE, 2011.
- [3] Ekso bionics website (2016). [Online]. Available: www.eksobionics.com
- [4] Cyberdyne inc. hal website (2016). [Online]. Available: www.cyberdyne.jp
- [5] S. Wang and H. van der Kooij, “Modeling, design, and optimization of mindwalker series elastic joint,” in *2013 IEEE International Conference on Rehabilitation Robotics June 24-26, 2013 Seattle, Washington USA*. IEEE, 2013.
- [6] N. Costa and D. G. Caldwell, “Control of a biomimetic soft-actuated 10dof lower body exoskeleton,” in *The First IEEE/RAS-EMBS International Conference on Biomedical Robotics and Biomechanics, 2006. BioRob 2006*. IEEE, 2006, pp. 495–501.
- [7] S.-H. Hyon *et al.*, “Design of hybrid drive exoskeleton robot xor2,” in *2013 IEEE/RSJ International Conference on Intelligent Robots and Systems (IROS)*, Nov 2013, pp. 4642–4648.
- [8] H. K. Kwa *et al.*, “Development of the ihmc mobility assist exoskeleton,” in *2009 IEEE International Conference on Robotics and Automation Kobe International Conference Center Kobe, Japan, May 12-17, 2009*. IEEE, 2009.
- [9] W. Yang *et al.*, “Design of an anthropomorphic lower extremity exoskeleton with compatible joints,” in *Proceedings of the 2014 IEEE International Conference on Robotics and Biomimetics*. IEEE, 2014.
- [10] J. L. Pons, “Rehabilitation exoskeletal robotics,” *Engineering in Medicine and Biology Magazine, IEEE*, vol. 29, no. 3, pp. 57–63, 2010.
- [11] M. Cempini *et al.*, “Self-alignment mechanisms for assistive wearable robots: A kinetostatic compatibility method,” *Robotics, IEEE Transactions on*, vol. 29, no. 1, pp. 236–250, 2013.
- [12] F. Giovacchini *et al.*, “A light-weight active orthosis for hip movement assistance,” *Robotics and Autonomous Systems*, vol. 73, pp. 123–134, 2015.
- [13] H. van der Kooij, “Design of a self-aligning 3-dof actuated exoskeleton for diagnosis and training of wrist and forearm after stroke,” in *International Conference on Rehabilitation Robotics*, 2013.
- [14] N. Vitiello *et al.*, “Neuroexos: A powered elbow exoskeleton for physical rehabilitation,” *IEEE Transactions on Robotics*, vol. 29, no. 1, pp. 220–235, 2013.
- [15] D. A. Neumann, *Kinesiology of the musculoskeletal system: foundations for rehabilitation*. Elsevier Health Sciences, 2013.
- [16] “Din 33402-2 (2005-12): Ergonomics - human body dimensions - part 2: Values,” Dec. 2005.
- [17] C. Mandery *et al.*, “The kit whole-body human motion database,” in *International Conference on Advanced Robotics (ICAR)*, July 2015, pp. 329–336.